Biochemistry and Biophysics Reports 22 (2020) 100754

Contents lists available at ScienceDirect

Biochemistry and Biophysics Reports

journal homepage: www.elsevier.com/locate/bbrep

Spermine synthesis inhibitor blocks 25-hydroxycholesterol-induced-apoptosis via SREBP2 upregulation in DLD-1 cell spheroids

Miku Kakimoto, Hideya Yamamoto, Arowu R. Tanaka*

Laboratory of Physiology and Morphology, Department of Life Sciences, School of Pharmacy, Yasuda Women's University, 6-13-1 Yasuhigashi, Asaminami Ward, Hiroshima City, Hiroshima, 731-0153, Japan

ARTICLE INFO

Keywords:
25-Hydroxycholesterol
Polyamine
DFMO
APCHA
SREBP2

ABSTRACT

The oxysterol 25-hydroxycholesterol (25-HC) has diverse physiological activities, including the ability to inhibit anchorage-independent growth of colorectal cancer cells. Here, we found that a polyamine synthesis inhibitor, DFMO, prevented 25-HC-induced apoptosis in non-anchored colorectal cancer DLD-1 cells. Additionally, we found that the spermine synthesis inhibitor APCHA also inhibited 25-HC-induced apoptosis in DLD-1 spheroids. Inhibiting the maturation of SREBP2, a critical regulator of cholesterol synthesis, reversed the effects of APCHA. SREBP2 knockdown also abolished the ability of APCHA to counteract 25-HC activity. Furthermore, APCHA induced SREBP2 maturation and upregulated its transcriptional activity, indicating that altered polyamine metabolism can increase SREBP2 activity and block 25-HC-induced apoptosis in spheroids. These results suggest that crosstalk between polyamine metabolism and cholesterol synthetic pathways via SREBP2 governs the proliferative and malignant properties of colorectal cancer cells.

1. Introduction

A growing number of physiological processes are regulated by the oxysterol 25-hydroxycholesterol (25-HC) [1]. In vivo, 25-HC is specifically produced from cholesterol by cholesterol 25-hydroxylase [2]. Meanwhile, it is non-specifically generated together with other oxysterols by the action of ROS generated in mitochondria [3]. It is also easily generated when foodstuffs rich in fat (such as meat) are cooked [4]. However, the mechanisms that control the generation of 25-HC (and those that determine the biological responses to its production) are not well understood.

Among the classical functions of 25-HC is its ability to negatively control de novo cholesterol synthesis [5,6]. SREBP2 (sterol regulatory element binding protein 2), which belongs to the basic-helix-loop-helix-leucine zipper (bHLH-Zip) family, is the master transcription factor for cholesterol synthesis and is produced as a membrane-bound precursor protein localized in the endoplasmic reticulum [7,8]. In the presence of excess cellular cholesterol, SREBP2 forms a dimer with SCAP (SREBP cleavage activating protein), which then binds to insulin inducing gene (INSIG), to form a trimer in the endoplasmic reticulum. When cholesterol content in cells is decreased, this trimerization is inhibited and the SREBP2-SCAP dimer is transported to the Golgi apparatus, where it is sequentially cleaved by proteolytic enzymes (S1P and S2P) around the membrane-binding site. The N-terminal fragment of SREBP2 then translocates to the nucleus, where it acts as a transcription factor for cholesterol synthesis. 25-HC inhibits the maturation and activation of SREBP2 by binding more tightly to SCAP and INSIG than cholesterol, thereby stopping de novo cholesterol synthesis [5,6].

Roles for 25-HC in addition to cholesterol metabolism are rapidly being elucidated, especially in cancer biology and immunology [9,10]. 25-HC can inhibit the entry of several viruses into cells [6,11,12]. We previously reported that 25-HC induces anoikis specifically in colorectal cancer cells [13]. Normally, when epithelial cells lose contact with extracellular matrix, they undergo a form of apoptosis called anoikis. However, cancer cells often undergo epithelial-mesenchymal transformation (EMT), which allows them to overcome anoikis and metastasize [14].

In this paper, we demonstrate that treatment with a spermine synthesis inhibitor, APCHA, induces SREBP2 maturation and increases its activation, thereby abrogating 25-HC-induced apoptosis in

Abbreviations: 25-HC, 25-hydroxycholesterol; SREBP2, sterol regulatory element binding protein 2; SCAP, SREBP cleavage activating protein; INSIG, insulin inducing gene; S1P, site-1 protease; S2P, site-2 protease; poly-HEMA, poly-(2-hydroxyethyl methacrylate); MTT, 3-[4,5-dimethylthiazol-2-yl]-2,5-diphenyltetrazolium bromide; DFMO, difluoromethylornithine; APCHA, N-(3-Aminopropyl)cyclohexylamine; SRE, sterol response element; HMG-CoA, 3-hydroxy-3-methylglutaryl-coenzyme A

* Corresponding author.
E-mail address: tanaka-a@yasuda-u.ac.jp (A.R. Tanaka).

https://doi.org/10.1016/j.bbrep.2020.100754
Received 16 October 2019; Received in revised form 13 March 2020; Accepted 14 March 2020

colorectal cancer DLD-1 cell spheroids. Chemical and genetic inactivation of SREBP2 abolished the prosurvival effect of APCHA. These results indicate that changes in polyamine metabolism affect cholesterol metabolism via SREBP2 in DLD-1 cell spheroids. They also suggest the involvement of polyamines in malignant transformation during the progression of colorectal cancer, and indicate that SREBP2 might be a new anticancer drug target.

2. Materials and methods

2.1. Cell culture, spheroids formation, and microscopy imaging

Human colorectal cancer DLD-1 cells (JRCB, Japan) were cultured in RPMI1640 medium supplemented with 10% fetal bovine serum and Penicillin (100U) – Streptomycin (100 μg/mL) solution at 37 °C in a 5% CO_2 incubator. For spheroid formation or anchorage-independent cell growth, culture plates were coated with poly-(2-hydroxyethyl methacrylate) (poly-HEMA, Sigma Aldrich). Coating was achieved by pouring 5 mg/mL poly-HEMA in 95% ethanol into culture plate wells and allowing it to completely evaporate in sterile condition. For spheroid formation, DLD-1 cells were seeded into poly-HEMA-coated round bottom 96 well plates (1×10^4 per well) and cultured for 72 h. DLD-1 cell spheroids were observed with a light microscope CKX-41 and photographed using DP25 digital camera (Olympus).

2.2. Measurement of anchorage-dependent or independent growth (MTT assay)

DLD-1 cells were seeded onto normal or poly-HEMA-coated flat bottom 96 well culture plates (1×10^4 per well) and treated with/without 25-hydroxycholesterol (25-HC, Sigma Aldrich) and/or difluoromethylornithine (DFMO, LKT laboratories or SCADS Inhibitor Kit, Screening Committee of Anticancer Drugs) and/or N-(3-Aminopropyl) cyclohexylamine (APCHA, Tokyo Chemical Industry, Japan) for 72 h. Cell growth was determined using 3-[4,5-dimethylthiazol-2-yl]-2,5-diphenyltetrazolium bromide (MTT, Roche) as described previously [15]. In brief, DLD-1 cells were treated with MTT for 4 h and dissolved with SDS overnight. The production of formazan due to reduction of MTT by living cells was measured at 570 nm using a spectrophotometer (ARVO MX model or Nivo, PerkinElmer).

2.3. Measurement of cell spheroid growth

DLD-1 cells were seeded onto poly-HEMA-coated round bottom 96 well culture plates (1×10^4 per well) and treated with/without 25-HC, N-(3-Aminopropyl)cyclohexylamine and/or PF-429242 (Cayman Chemical) for 72 h. Cell spheroid growth was determined using the Cell Titer Glo 3D Cell Viability Assay kit (Promega) according to the manufacturer's instructions. The luminescence was measured by a luminometer ARVO MX model or Nivo (PerkinElmer) using white flat bottom 96 well plates (Thermo Scientific).

2.4. RNA interference assay

DLD-1 cells on normal 6-well plates were transfected with siRNAs (5 nM) using Lipofectamine RNAi MAX (Invitrogen). Silencer Negative Control #1 (AM4611) and SREBP2-specific siRNA (s27) (Ambion) were used. After incubation for 24 h, cells were collected for immunoblot analysis. For spheroid formation, transfected cells were trypsinized and resuspended in the same medium. Resuspended cells were plated onto poly-HEMA-coated round-bottom plates (1×10^4 per well) with/without 25-HC and/or APCHA. After incubation for 72 h, spheroid growth was determined using the Cell Titer Glo 3D Cell Viability assay as above.

2.5. Immunoblot analysis

DLD-1 cells were seeded onto poly-HEMA-coated flat bottom 6 well plates (2×10^5 per well), and then treated with APCHA at different concentrations for 24 h. These cells and the siRNA-transfected cells described above were washed with cold PBS buffer. The cells were then lysed via sonication on ice in RIPA buffer (Fujifilm Wako) containing protease inhibitors (Roche). Total protein content was measured using a BCA Protein Assay Kit (Pierce). Equal amounts of protein were subjected to SDS-PAGE gel, electrophoresed, and transferred onto PVDF membrane. Membranes were blocked with fraction V BSA and incubated overnight with primary antibodies against SREBP2 (MBL, Japan) or β-actin (Fujifilm Wako). Membranes were washed and incubated with secondary goat anti-mouse IgG conjugated with HRP (MBL). Chemiluminescence signals generated with ECL plus (GE Healthcare) were detected using a luminoimage analyzer LAS4000 (GE Healthcare).

2.6. Dual luciferase reporter assay

DLD-1 cells were seeded onto poly-HEMA-coated flat bottom 96 well culture white plates (0.5×10^4 per well) (SPL Life Sciences, Korea) and transfected with pSynSRE-T-Luc (45 ng per well) (Addgene) and 5 ng pKM2L-pvCMV (5 ng per well) (RIKEN BRC through the National BioResource Project of the MEXT/AMED, Japan) using Lipofectamine 3000 (Invitrogen), and treated with Rosuvastatin (Fujifilm Wako) or APCHA for 24 h. The firefly luciferase activity of pSynSRE-T-Luc and Renilla luciferase activity of pKM2L-pvCMV for normalization were detected by a luminophotometer Nivo using the Dual-Glo Luciferase Assay System (Promega) according to the manufacturer's instructions.

2.7. Quantification of 25-HC in mouse feces

Mouse (BALB/c, 8 weeks, n = 6) feces were collected randomly and dissolved in methanol-KOH (5:2, v/v). After 1 h hard mixing, 50% phosphate, water and hexane were added sequentially. These solutions were centrifuged at 3000 rpm. The hexane layers were cleaned up by Solid Phase Extraction (Bond Elut SI, Agilent Technologies). Fresh hexane and hexane-ethyl acetate (9:1, v/v) solutions were added sequentially. Fresh ethyl acetate was added into the eluted oxysterols and evaporated under stream nitrogen. Samples were resuspended in ethanol and measured by LC-MS (LCMS-8040, Shimadzu). An absolute calibration method was used to quantify 25-HC.

2.8. Statistical analysis

Data are presented as mean ± SEM (standard error of the mean). Dunnett's test was for the statistical comparison of the differences between control and other groups. Tukey's test was performed for the statistical comparison of the differences between all groups. All analyses were performed using BellCurve for Excel (Social Survey Research Information, Japan).

3. Results

3.1. Polyamine synthesis inhibitors block apoptosis induced by 25-hydroxycholesterol in non-anchored or spheroid DLD-1 cells

We previously reported that 25-HC induced anoikis, a form of detachment-induced apoptosis, through the p38 MAPK pathway in colorectal cancer DLD-1 cells [13]. To determine whether 25-HC is present under physiological conditions, we measured its abundance in mouse feces and confirmed that is was readily detectable (820 ± 111 μg/kg). This suggests that 25-HC may slow down the development and progression of colorectal cancer, because feces could be directly exposed to the malignant cells.

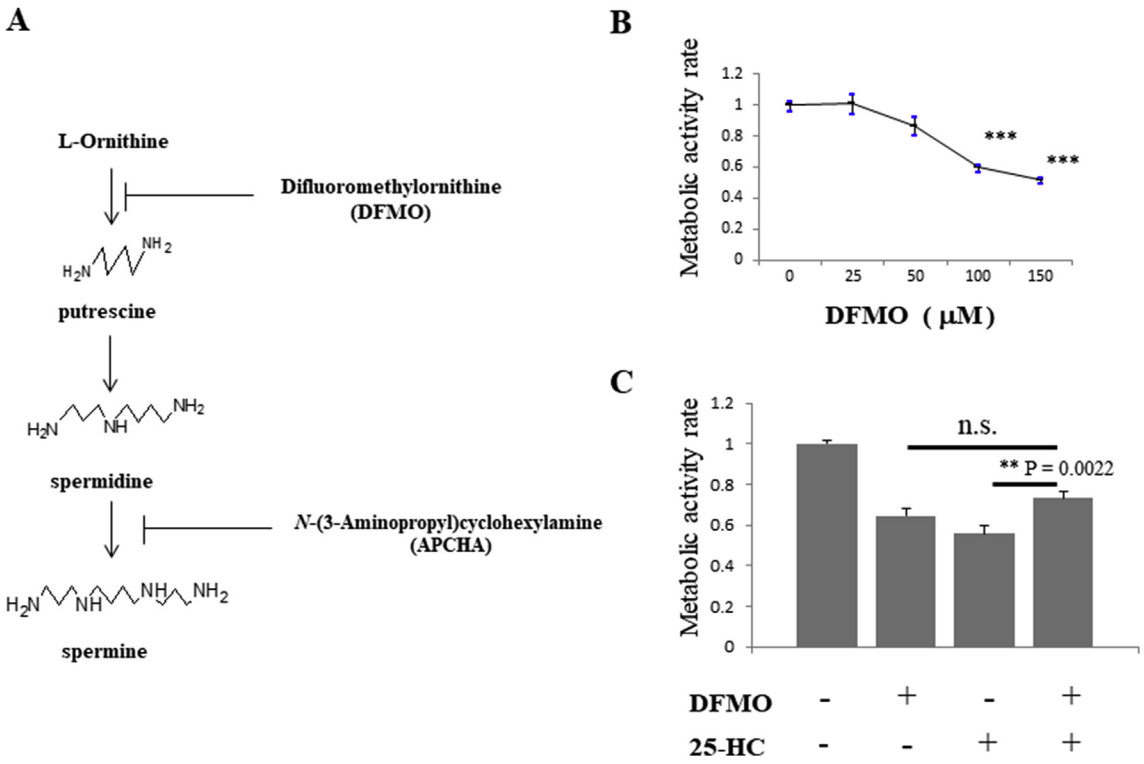

Fig. 1. DFMO partially inhibits apoptosis induced by 25-HC in non-anchored DLD-1 cells.
A. Polyamine synthesis pathway. **B.** DFMO inhibits the cell growth of non-anchored DLD-1 cells in a concentration-dependent manner. The survival rate of cells treated with vehicle was designated as 1.00. Each plot represents the means of three independent experiments (each of which had triplicate data points). **C.** Concurrent treatment of non-anchored DLD-1 cells with DFMO (100 μM) showed the partial inhibition of apoptosis induced by 25-HC (1 μM). Each plot represents the mean of four independent experiments (each of which had triplicate data points). All data show the mean ± SEM. Dunnett's test was performed in Fig. 1B and Tukey's test was performed in Fig. 1C; ***P < 0.001.

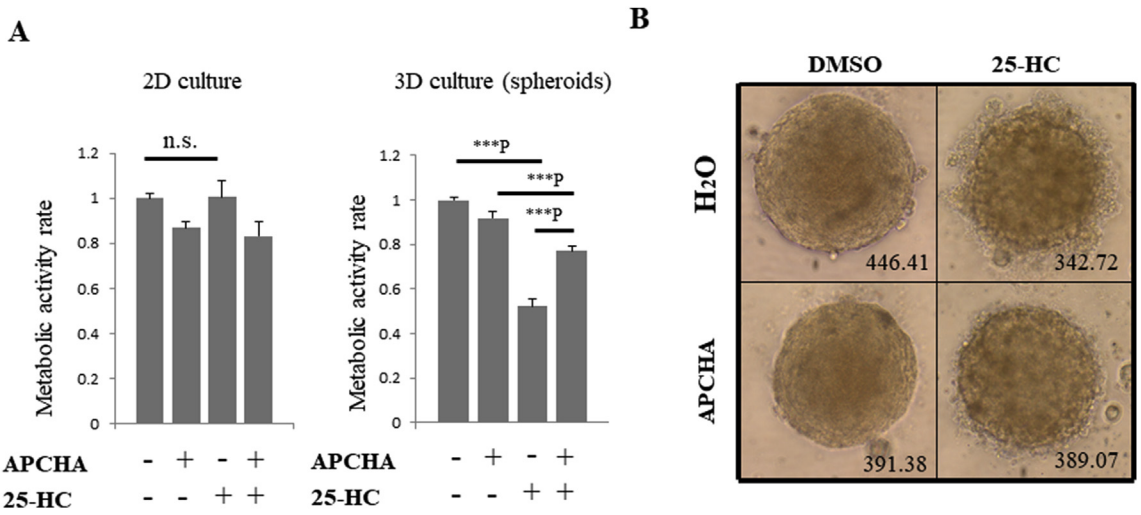

Fig. 2. APCHA treatment attenuates 25-HC-induced apoptosis in DLD-1 spheroids.
A. Effects of 25-HC (1 μM) and/or APCHA (300 μM) on DLD-1 cells in 2D or 3D. Each plot represents the means of four independent experiments (each of which had triplicate data points). All data show the mean ± SEM. Tukey's test was performed. ***P indicates P < 0.001. **B.** Morphological effects of a 72-h treatment of DLD-1 spheroids with 25-HC (1 μM) and/or APCHA (300 μM). Diameter (μm) of spheroids is indicated.

To further investigate the mechanism of 25-HC-induced apoptosis, we screened for compounds that were able to inhibit the process in non-anchored DLD-1 cells. We identified difluoromethylornithine (DFMO), an inhibitor of ornithine decarboxylase (ODC), which is the rate-limiting enzyme of polyamine synthesis (Fig. 1A). Elevated polyamine synthesis is present in some malignancies, including colorectal cancer, and correlates with malignancy; these observations have triggered many studies into the potential of DFMO as an anticancer agent [16]. In fact, DFMO also inhibited anchorage-independent growth of DLD-1 cells in a dose-dependent manner (Fig. 1B). Surprisingly, we discovered that DFMO reduced 25-HC-induced apoptosis from 44% to 27%. However, treatment with DFMO alone also reduced viability by 36% (Fig. 1C). There was a statistical difference between the 25-HC and DFMO +25-HC treatments, but no statistical difference between the DFMO and DFMO +25-HC treatments. These results suggest that the ability of DFMO to inhibit 25-HC-induced apoptosis is masked by the

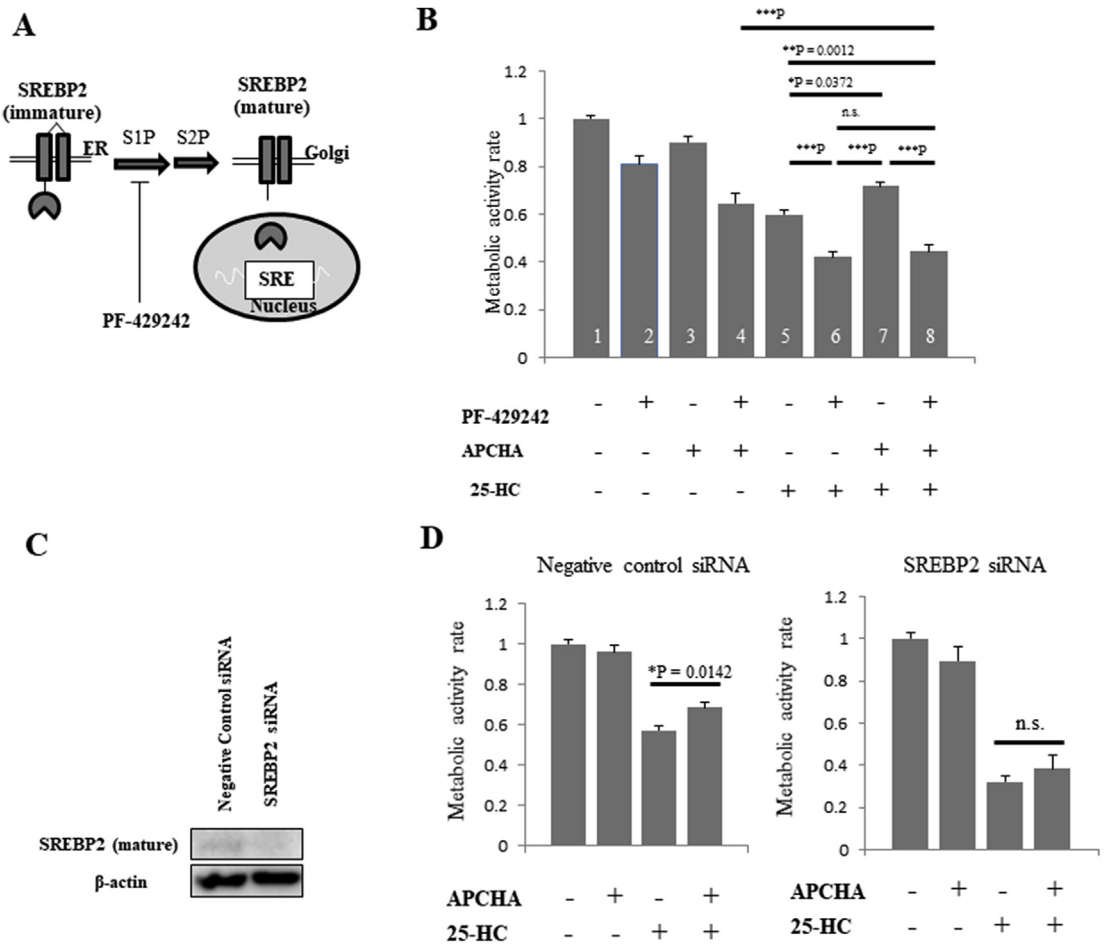

Fig. 3. Downregulation of SREBP2 inhibits 25-HC-induced apoptosis in DLD-1 cell spheroids.
A. SREBP2 activation pathway. Immature SREBP2 is digested sequentially by S1P and S2P, whereupon mature SREBP2 translocates to the nucleus and binds to sterol response element (SRE) sites on chromosomes. PF-429242 is a specific S1P inhibitor. **B.** Treatment of DLD-1 cell spheroids with PF-429242 (10 μM), APCHA (300 μM) and/or 25-HC (1 μM). Each plot represents the mean of seven independent experiments (each of which had triplicate data points). All data show the mean ± SEM. Tukey's test was performed. *P, **P and ***P indicate $P < 0.05$, $P < 0.01$ and $P < 0.001$, respectively. **C.** SREBP2 gene knockdown. SREBP2-specific siRNA or negative control siRNA was transfected into non-anchored DLD-1 cells for 24 h. Cell lysates were electrophoresed through 10% SDS-PAGE, and then subjected to immunoblotting using anti-SREBP2 or anti-β-actin antibodies. **D.** DLD-1 spheroids transfected with negative control siRNA (left) or SREBP2 siRNA (right) were treated with 25-HC (1 μM) and/or APCHA (300 μM). Each plot represents the mean of four independent experiments (each of which had triplicate data points). All data show the mean ± SEM. Tukey's test was performed.

anti-proliferative effects of DFMO itself.

To overcome the limitations of DFMO as an inhibitor of all polyamine biosynthesis, we used N-(3-Aminopropyl)cyclohexylamine (APCHA), which selectively inhibits spermine synthase (Fig. 1A) [17]. In addition, we used three-dimensional multicellular tumor DLD-1 spheroids formed in poly-HEMA-coated round bottom plates in order to prevent variations in treatment responses and to standardize spheroid size and morphology [18]. As a result, treatment with 25-HC reduced the viability of DLD-1 cell spheroids to about 52%, but simultaneous treatment with APCHA and 25-HC restored viability to 77% (Fig. 2A, right), while treatment with 25-HC had no effect on the viability of DLD-1 cells in normal two-dimensional (2D) culture condition (Fig. 2A, left). Treatment with APCHA alone restored survival to approximately 92% and was associated with significantly less toxicity when compared to DFMO ($p < 0.01$) in DLD-1 spheroids. Furthermore, bubble-like dead cells were observed around spheroids after treatment with 25-HC (Fig. 2B, upper right panel), whereas this phenotype was suppressed by APCHA co-treatment (Fig. 2B, lower right panel). These results suggest that selective inhibition of polyamine synthesis can attenuate 25-HC-induced apoptosis in DLD-1 cell spheroids.

3.2. APCHA inhibits apoptosis induced by 25-hydroxycholesterol via SREBP2 activation

We surmised that inhibition of polyamine synthesis (especially APCHA-dependent inhibition of spermine synthesis and the consequent reduction of the spermine/spermidine ratio) could attenuate 25-HC-dependent cell death by three different mechanisms. For example, APCHA might reduce pro-apoptotic signaling, or increase survival signaling. Alternatively, APCHA might reduce the intracellular concentrations of 25-HC. Recently, sterol regulatory element binding protein 2 (SREBP2), the master regulator of cholesterol synthesis, and its activator, site-1 protease (S1P), were suggested as metabolic targets in glioblastoma and colorectal cancer (Fig. 3A) [19,20]. We inferred that APCHA might increase SREBP2 activity and therefore increase survival cell signaling and reduce intracellular 25-HC; indeed, SREBP2 upregulates cholesterol synthesis and decreases the intracellular 25-HC/cholesterol ratio. Here, we used PF429242, a specific S1P inhibitor, to elucidate the involvement of SREBP2 in 25-HC-induced apoptosis in DLD-1 spheroids. Indeed, PF429242 abrogated the protective effects of APCHA (Fig. 3B, graph bars 7 and 8), and 25-HC-induced apoptosis was actually enhanced by treatment with PF429242 (Fig. 3B, graph bars 5 and 6). These results suggest that activation of SREBP2 might mediate

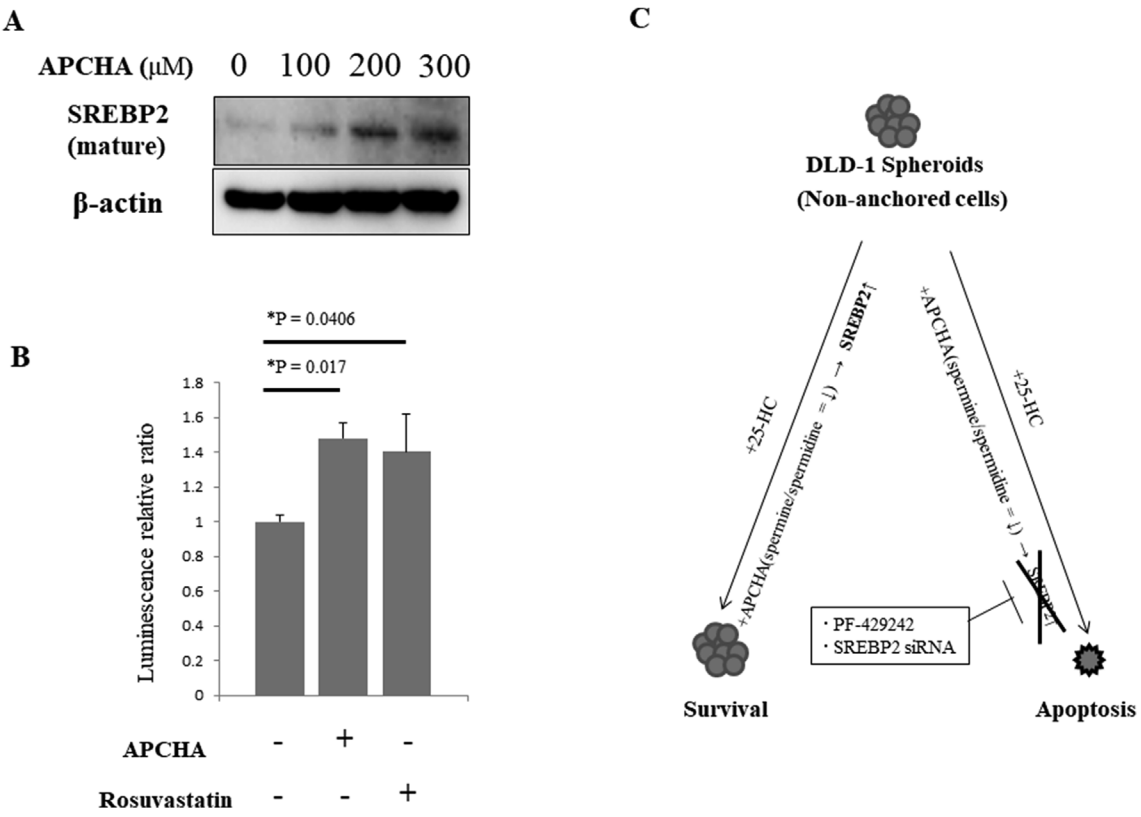

Fig. 4. APCHA increases SREBP2 maturation and activity in non-anchored DLD-1 cells.
A. APCHA treatment increases mature SREBP2 in a dose-dependent manner. Non-anchored DLD-1 cells were treated with APCHA at the indicated concentrations, lysed and electrophoresed through 10% SDS-PAGE, and then subjected to immunoblotting using anti-SREBP2 or anti-β-actin antibodies. **B.** Transcriptional activation of Sterol Response Element (SRE) by APCHA. pSynSRE-T-Luc and pKM2L-pvCMV were transfected into non-anchored DLD-1 cells and treated with DMSO (negative control), APCHA (300 μM) or Rosuvastatin (2.5 μM; positive control) for 24 h. Firefly luciferase activity (SRE transcriptional activity) and Renilla luciferase activity (internal control) were detected. Each plot represents the mean of four independent experiments (each of which had triplicate data points). All data show the mean ± SEM. Dunnett's test was performed. **C.** APCHA-dependent upregulation of SREBP2 prevents apoptosis induced by 25-HC in DLD-1 cell spheroids. Treatment with APCHA may decrease the spermine/spermidine ratio, thereby upregulating SREBP2 activity and rescuing cancer cells from 25-HC-induced apoptosis. Conversely, chemical and genetic inhibition of SREBP2 abolishes the effect of APCHA, leading to increased cell death following 25-HC treatment.

the protective effects of APCHA.

Next, we knocked down SREBP2 expression using a specific siRNA, and observed a reduction in SREBP2 in nearly all non-anchored DLD-1 cells (Fig. 3C). We found that, when compared to control non-targeting siRNA, SREBP2 knockdown prevented the anti-apoptotic effects of APCHA (Fig. 3D). These results indicate that SREBP2 counteracts the effects of 25-HC and may mediate the protective effect of APCHA with regard to 25-HC-induced apoptosis.

Finally, we examined whether APCHA regulated the expression or activity of SREBP2. Indeed, the mature form of SREBP2 was increased by APCHA in a concentration-dependent manner (Fig. 4A). In addition, we examined whether APCHA increased the transcriptional activation of sterol response element (SRE), which is upregulated by SREBP2. Accordingly, the transcriptional activity of SRE was increased by 1.5-fold relative to control cells in the presence of APCHA, and by 1.4-fold in the presence of the positive control Rosuvastatin, an HMG-CoA reductase inhibitor (Fig. 4B). These results suggest that APCHA directly activates the expression, maturation and transcriptional activation of SREBP2.

4. Discussion

In this study, we found that the polyamine synthesis inhibitors DFMO and APCHA attenuate 25-HC-induced apoptosis in colorectal cancer DLD-1 cells in an SREBP2-dependent manner. Inhibiting SREBP2 (both chemically and genetically) abolished the effect of APCHA treatment. We also found that APCHA increased mature SREBP2 protein and increased the activity of SREBP2-responsive promoters.

Polyamines are a diverse set of polycationic alkylamines in mammalian cells, with putrescine, spermidine and spermine being particularly abundant [21]. Among their many functions, polyamines are essential for cell survival and proliferation [22]. DFMO, which inhibits all polyamine synthesis, is a potential anticancer agent [16]. Diacetylspermine, a diacetylated form of spermine, has attracted attention as a marker of colorectal cancer in the urine, and polyamine metabolism is implicated in the growth and progression of colorectal cancer [23]. APCHA, an intermediate inhibitor of polyamine synthesis, inhibited 25-HC-induced apoptosis of DLD-1 cell spheroids, a phenomenon not observed when the cells were cultured in 2D. Thus, the effects of polyamines in tumor cells are heavily context-dependent. We did attempt to show a direct role for polyamines in 25-HC-induced apoptosis, but the results were inconclusive (data not shown). Although the reasons for this remain unclear, we speculate that hydrophilic polyamines and hydrophobic 25-HC and APCHA may be absorbed with different efficiencies in the central part of spheroids.

Previously, we discovered that 25-HC-induced anoikis was inhibited by Y27632 treatment, a Rho-associated protein kinase inhibitor [13]. Therefore, we speculate that the sensitivity of 25-HC is influenced by properties of the cytoskeleton that vary according to 3D, anchorage-independent or 2D culture conditions. The effect of polyamines on DLD-1 cells may be influenced by the status of the cytoskeleton in a similar manner.

Although it is unclear why inhibition of spermine synthase by APCHA activates SREBP2, we suggest that a reduced spermine/

spermidine ratio or altered polyamine composition may play critical roles. Among the polyamines, spermidine is particularly important for cell growth, and is also an activator of autophagy [24,25]. Meanwhile, in nutrient-deficient HeLa cells, SREBP2 induces autophagy-related genes and is required for the formation of autophagosomes [26]. Taken together, the APCHA-dependent increase of spermidine due to spermine synthase inhibition may contribute to activation of SREBP2 through the autophagic pathway. Interestingly, 25-HC has the opposite effect in breast cancer, where it promotes cell proliferation and progression [27]. This is because 25-HC stimulates estrogen receptor α in a breast cancer-specific manner and generates proliferative signals. This effect is more pronounced with 27-HC, an oxidized sterol related to 25-HC [28,29]. Recently, Ortiz et al. reported that exosomes from melanoma downregulated cholesterol 25-hydroxylase in normal cells, which in turn reduces 25-HC production; the authors suggested that normal cells are more likely to convert to a pre-metastatic niche by taking up exosomes from melanoma [30]. These diverse observations indicate that the response of normal and cancer cells to 25-HC is highly context-dependent.

SREBP2 is upregulated in cancer cells and contributes to the malignant transformation of cancer [8]. Wen et al. reported that knockdown of SREBP suppressed the growth of colorectal cancer cells [20]. Here, we found that inhibition or knockdown of SREBP2 increased susceptibility to 25-HC, and that APCHA decreased 25-HC-induced apoptosis by increasing SREBP2 activity. Taken together, these data support the hypothesis that SREBP2 is a potential target for cancer therapy. We conclude that 25-HC-driven apoptosis in DLD-1 colorectal cancer cell spheroids is modulated by alterations in polyamine metabolism. In line with this, altered polyamine metabolism affected the activation state of SREBP2 (Fig. 4C). These results provide new insight into the importance of SREBP2 as a cellular node connecting polyamine and cholesterol metabolism in colorectal cancer growth.

Author statement

A.R.T. designed and directed the project. M.K., H.Y. and A.R.T. contributed to the design and implementation of the research, to the analysis of the results and to the writing of the manuscript.

Declaration of competing interest

The authors declare no competing financial interest.

Acknowledgements / grant support

Financial support for this study was provided by Ministry of Education, Culture, Sports, Science and Technology of Japan (15K16224 and 25221203) to ART. Material support for this study was provided by Screening Committee of Anticancer Drugs supported by Grant-in-Aid for Scientific Research on Innovative Areas, Scientific Support Programs for Cancer Research, from the Ministry of Education, Culture, Sports, Science and Technology, Japan.

References

[1] W.J. Griffiths, Y. Wang, An update on oxysterol biochemistry: new discoveries in lipidomics, Biochem. Biophys. Res. Commun. 504 (2018) 617–622, https://doi.org/10.1016/j.bbrc.2018.02.019.

[2] E.G. Lund, T.A. Kerr, J. Sakai, W.P. Li, D.W. Russell, cDNA cloning of mouse and human cholesterol 25-hydroxylases, polytopic membrane proteins that synthesize a potent oxysterol regulator of lipid metabolism, J. Biol. Chem. 273 (1998) 34316–34327, https://doi.org/10.1074/jbc.273.51.34316.

[3] A.J. Brown, W. Jessup, Oxysterols: sources, cellular storage and metabolism, and new insights into their roles in cholesterol homeostasis, Mol. Aspect. Med. 30 (2009) 111–122, https://doi.org/10.1016/j.mam.2009.02.005.

[4] J.-S. Min, M.I. Khan, S.-O. Lee, D.G. Yim, K.H. Seol, M. Lee, C. Jo, Impact of cooking, storage, and reheating conditions on the formation of cholesterol oxidation products in pork loin, Korean J. Food Sci. Anim. Resour. 36 (2016) 23–28, https://doi.org/10.5851/kosfa.2016.36.1.23.

[5] M.S. Brown, A. Radhakrishnan, J.L. Goldstein, Retrospective on cholesterol homeostasis: the central role of scap, Annu. Rev. Biochem. 87 (2017) 783–807, https://doi.org/10.1146/annurev-biochem-062917-011852.

[6] D. Lembo, V. Cagno, A. Civra, G. Poli, Oxysterols: an emerging class of broad spectrum antiviral effectors, Mol. Aspect. Med. 49 (2016) 23–30, https://doi.org/10.1016/j.mam.2016.04.003.

[7] H. Shimano, R. Sato, SREBP-regulated lipid metabolism: convergent physiology — divergent pathophysiology, Nat. Rev. Endocrinol. 13 (2017) 710–730, https://doi.org/10.1038/nrendo.2017.91.

[8] X. Cheng, J. Li, D. Guo, SCAP/SREBPs are central players in lipid metabolism and novel metabolic targets in cancer therapy, Curr. Top. Med. Chem. 18 (2018) 484–493, https://doi.org/10.4172/2157-7633.1000305.Improved.

[9] S.Y. Bah, P. Dickinson, T. Forster, B. Kampmann, P. Ghazal, Immune oxysterols: role in mycobacterial infection and inflammation, J. Steroid Biochem. Mol. Biol. 169 (2017) 152–163, https://doi.org/10.1016/j.jsbmb.2016.04.015.

[10] A. Kloudova, F.P. Guengerich, P. Soucek, The role of oxysterols in human cancer, Trends Endocrinol. Metabol. 28 (2017) 485–496, https://doi.org/10.1016/j.tem.2017.03.002.

[11] P. Shrivastava-ranjan, É. Bergeron, A.K. Chakrabarti, C.G. Albariño, M. Flint, S.T. Nichol, 25-Hydroxycholesterol inhibition of lassa virus infection through, mBio 7 (2016) 1–9, https://doi.org/10.1128/mBio.01808-16.

[12] C. Li, Y.Q. Deng, S. Wang, F. Ma, R. Aliyari, X.Y. Huang, N.N. Zhang, M. Watanabe, H.L. Dong, P. Liu, X.F. Li, Q. Ye, M. Tian, S. Hong, J. Fan, H. Zhao, L. Li, N. Vishlaghi, J.E. Buth, C. Au, Y. Liu, N. Lu, P. Du, F.X.F. Qin, B. Zhang, D. Gong, X. Dai, R. Sun, B.G. Novitch, Z. Xu, C.F. Qin, G. Cheng, 25-Hydroxycholesterol protects host against zika virus infection and its associated microcephaly in a mouse model, Immunity 46 (2017) 446–456, https://doi.org/10.1016/j.immuni.2017.02.012.

[13] A.R. Tanaka, K. Noguchi, H. Fukazawa, Y. Igarashi, H. Arai, Y. Uehara, P38MAPK and Rho-dependent kinase are involved in anoikis induced by anicequol or 25-hydroxycholesterol in DLD-1 colon cancer cells, Biochem. Biophys. Res. Commun. 430 (2013) 1240–1245, https://doi.org/10.1016/j.bbrc.2012.12.067.

[14] P. Paoli, E. Giannoni, P. Chiarugi, Anoikis molecular pathways and its role in cancer progression, Biochim. Biophys. Acta Mol. Cell Res. 1833 (2013) 3481–3498, https://doi.org/10.1016/j.bbamcr.2013.06.026.

[15] H. Fukazawa, S. Mizuno, Y. Uehara, A microplate assay for quantitation of anchorage-independent growth of transformed cells, Anal. Biochem. 228 (1995) 83–90, https://doi.org/10.1006/abio.1995.1318.

[16] G.A. Alexiou, G.D. Lianos, V. Ragos, V. Galani, A.P. Kyritsis, Difluoromethylornithine in cancer: new advances, Futur. Oncol. 13 (2017) 809–819, https://doi.org/10.2217/fon-2016-0266.

[17] K. Nishimura, K. Murozumi, A. Shirahata, M.H. Park, K. Kashiwagi, K. Igarashi, Independent roles of eIF5A and polyamines in cell proliferation, Biochem. J. 385 (2005) 779–785, https://doi.org/10.1042/bj20041477.

[18] S. Sant, P.A. Johnston, The production of 3D tumor spheroids for cancer drug discovery, Drug Discov. Today Technol. 23 (2017) 27–36, https://doi.org/10.1016/j.ddtec.2017.03.002.

[19] B.T. Caruana, A. Skoric, A.J. Brown, L.H. Lutze-Mann, Site-1 protease, a novel metabolic target for glioblastoma, Biochem. Biophys. Res. Commun. 490 (2017) 760–766, https://doi.org/10.1016/j.bbrc.2017.06.114.

[20] Y.A. Wen, X. Xiong, Y.Y. Zaytseva, D.L. Napier, E. Vallee, A.T. Li, C. Wang, H.L. Weiss, B.M. Evers, T. Gao, Downregulation of SREBP inhibits tumor growth and initiation by altering cellular metabolism in colon cancer article, Cell Death Dis. 9 (2018), https://doi.org/10.1038/s41419-018-0330-6.

[21] A.E. Pegg, R.A. Casero Jr., Current status of the polyamine research field, Methods Mol. Biol. 1 (2011) 3–35, https://doi.org/10.1016/B978-0-12-394807-6.00109-X.

[22] R.A.C. Jr, T.M. Stewart, A.E. Pegg, Polyamine metabolism and cancer: treatments, challenges and opportunities, Nat. Rev. Canc. 18 (2018) 681–695, https://doi.org/10.1038/s41568-018-0050-3.

[23] T. Nakajima, K. Katsumata, H. Kuwabara, R. Soya, M. Enomoto, T. Ishizaki, A. Tsuchida, M. Mori, K. Hiwatari, T. Soga, M. Tomita, M. Sugimoto, Urinary polyamine biomarker panels with machine-learning differentiated colorectal cancers, benign disease, and healthy controls, Int. J. Mol. Sci. 19 (2018) 1–14, https://doi.org/10.3390/ijms19030756.

[24] F. Pietrocola, S. Lachkar, D.P. Enot, M. Niso-Santano, J.M. Bravo-San Pedro, V. Sica, V. Izzo, M.C. Maiuri, F. Madeo, G. Mariño, G. Kroemer, Spermidine induces autophagy by inhibiting the acetyltransferase EP300, Cell Death Differ. 22 (2015) 509–516, https://doi.org/10.1038/cdd.2014.215.

[25] E. Morselli, G. Mariño, M.V. Bennetzen, T. Eisenberg, E. Megalou, S. Schroeder, S. Cabrera, P. Bénit, P. Rustin, A. Criollo, O. Kepp, L. Galluzzi, S. Shen, S.A. Malik, M.C. Maiuri, Y. Horio, C. López-Otín, J.S. Andersen, N. Tavernarakis, F. Madeo, G. Kroemer, Spermidine and resveratrol induce autophagy by distinct pathways converging on the acetylproteome, J. Cell Biol. 192 (2011) 615–629, https://doi.org/10.1083/jcb.201008167.

[26] Y.K. Seo, T. Il Jeon, H.K. Chong, J. Biesinger, X. Xie, T.F. Osborne, Genome-wide localization of SREBP-2 in hepatic chromatin predicts a role in autophagy, Cell Metabol. 13 (2011) 367–375, https://doi.org/10.1016/j.cmet.2011.03.005.

[27] R. Lappano, A.G. Recchia, E.M. de Francesco, T. Angelone, M.C. Cerra, D. Picard, M. Maggiolini, The cholesterol metabolite 25-Hydroxycholesterol activates estrogen receptor α-Mediated signaling in cancer cells and in cardiomyocytes, PloS One 6 (2011), https://doi.org/10.1371/journal.pone.0016631.

[28] M. Umetani, H. Domoto, A.K. Gormley, I.S. Yuhanna, C.L. Cummins, N.B. Javitt, K.S. Korach, P.W. Shaul, D.J. Mangelsdorf, 27-Hydroxycholesterol is an endogenous SERM that inhibits the cardiovascular effects of estrogen, Nat. Med. 13 (2007) 1185–1192, https://doi.org/10.1038/nm1641.

[29] E.R. Nelson, S.E. Wardell, J.S. Jasper, S. Park, S. Suchindran, M.K. Howe, N.J. Carver, R. V Pillai, P.M. Sullivan, V. Sondhi, U. Michihisa, J. Geradts, D.P. McDonnel, 27-Hydroxycholesterol links hypercholesterolemia and breast cancer pathophysiology, Science (80-.) 342 (2013) 1094–1098, https://doi.org/10.1126/science.1241908.

[30] A. Ortiz, J. Gui, F. Zahedi, P. Yu, C. Cho, S. Bhattacharya, C.J. Carbone, Q. Yu, K.V. Katlinski, Y.V. Katlinskaya, S. Handa, V. Haas, S.W. Volk, A.K. Brice, K. Wals, N.J. Matheson, R. Antrobus, S. Ludwig, S.Y. Fuchs, An interferon-driven oxysterol-based defense against tumor-derived extracellular vesicles, Canc. Cell 35 (2019) 33–45, https://doi.org/10.1016/j.ccell.2018.12.001.